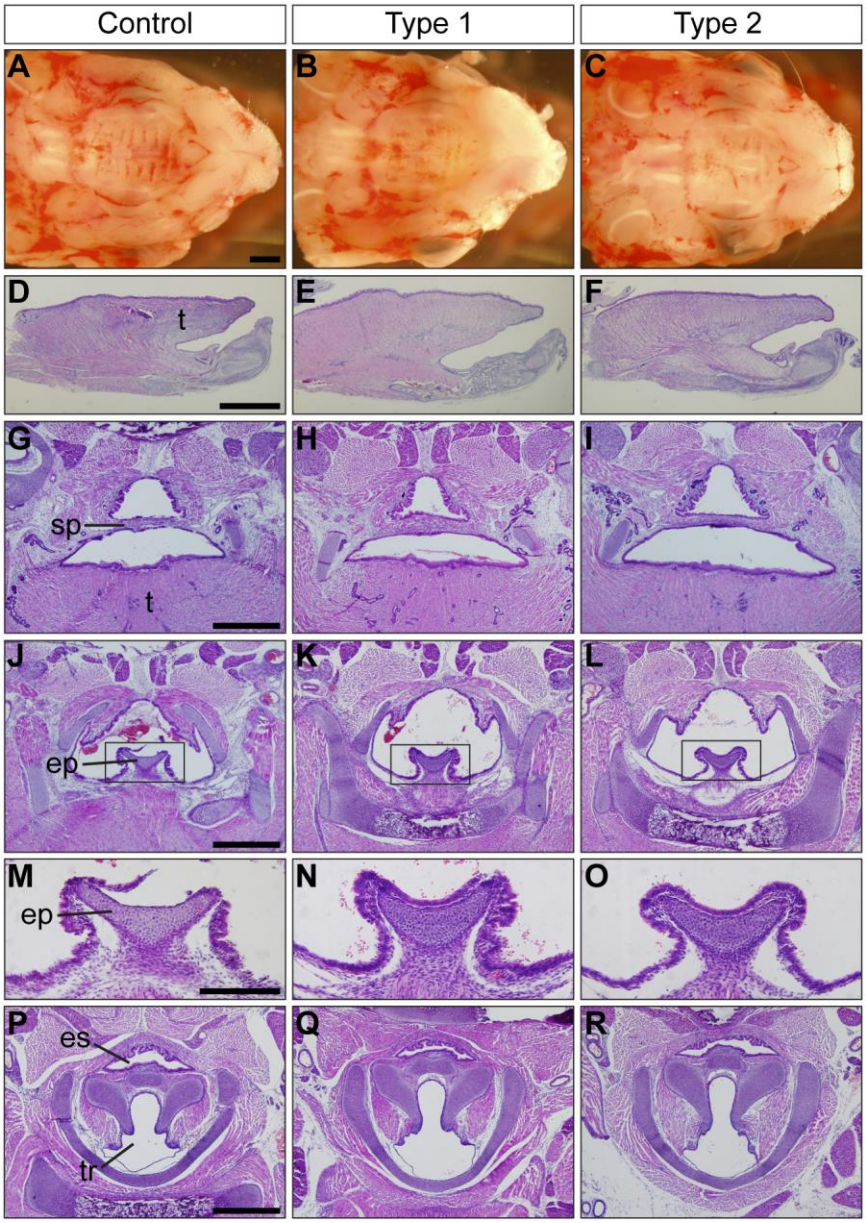

Supplementary Figure 1. No overt phenotype observed in palate, tongue, pharynx, or mandible of type 1 and type 2 mutants. (**A**-**C**) Palatal view of newborn control, type 1, and type 2 mutants after removal of mandible. No mutant showed cleft palate. Scale bar: 1 mm. (**D**-**R**) Hematoxylin and eosin (H&E) staining of newborn pups. Sagittal sections of the tongue (D-F) and coronal sections of the pharynx (G-R) of each group revealed no overt abnormalities in both type 1 and type 2 mutant respiratory organs. Boxed areas in J,K, and L are shown at higher magnification in M,N, and O respectively. Scale bars in D: 1mm. G,J,P: 500 μm. M: 200 μm. t, tongue; sp, soft palate; ep, epiglottis; es, esophagus; tr, trachea.

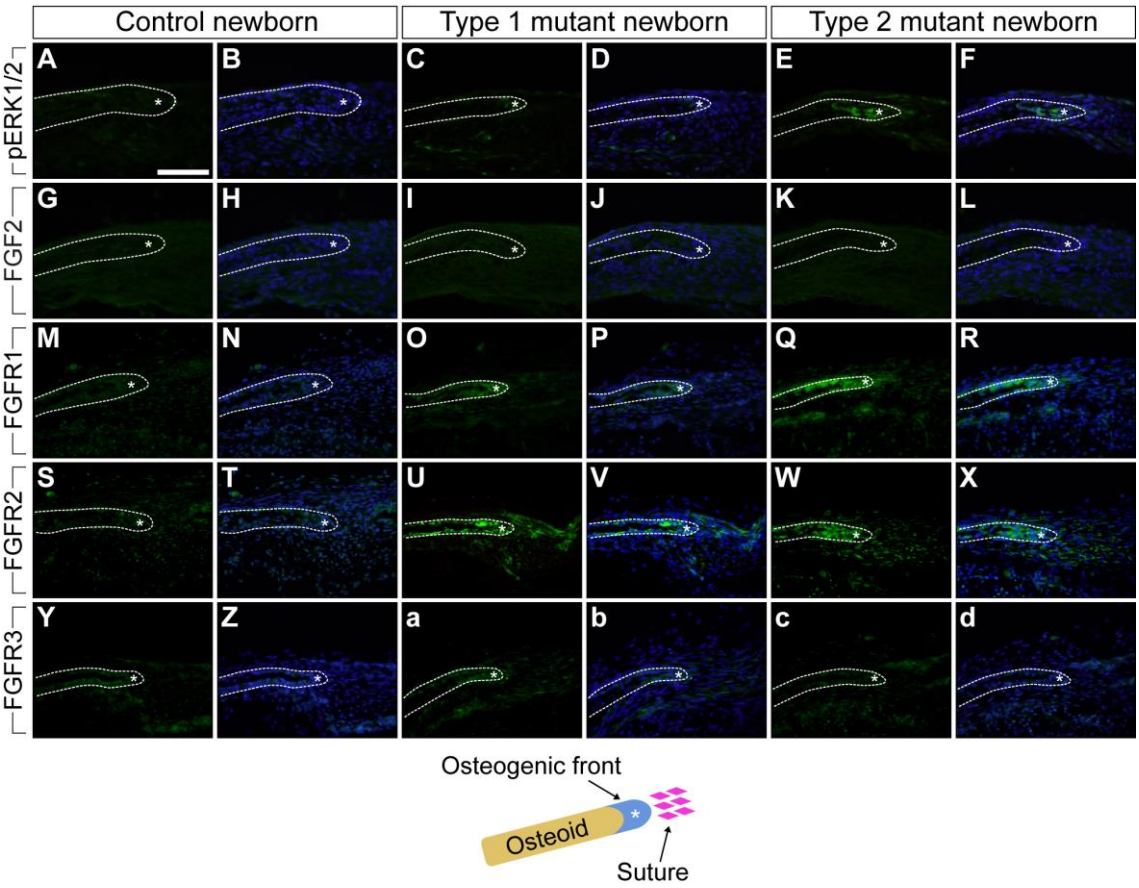

Supplementary Figure 2. FGF signaling components were upregulated in the anterior frontal suture of newborn mutants. (**A-Z, a-d**) Immunohistochemistry was performed using pERK1/2, FGF2, FGFR1, FGFR2, and FGFR3 antibodies (green). The levels of FGFR1 and FGFR2 were upregulated in the anterior frontal suture and osteogenic front of both mutants (O-R, U-X). In these images blue indicates DAPI signal. Osteogenic front is marked by white asterisks. Scale bar: 100 μm.

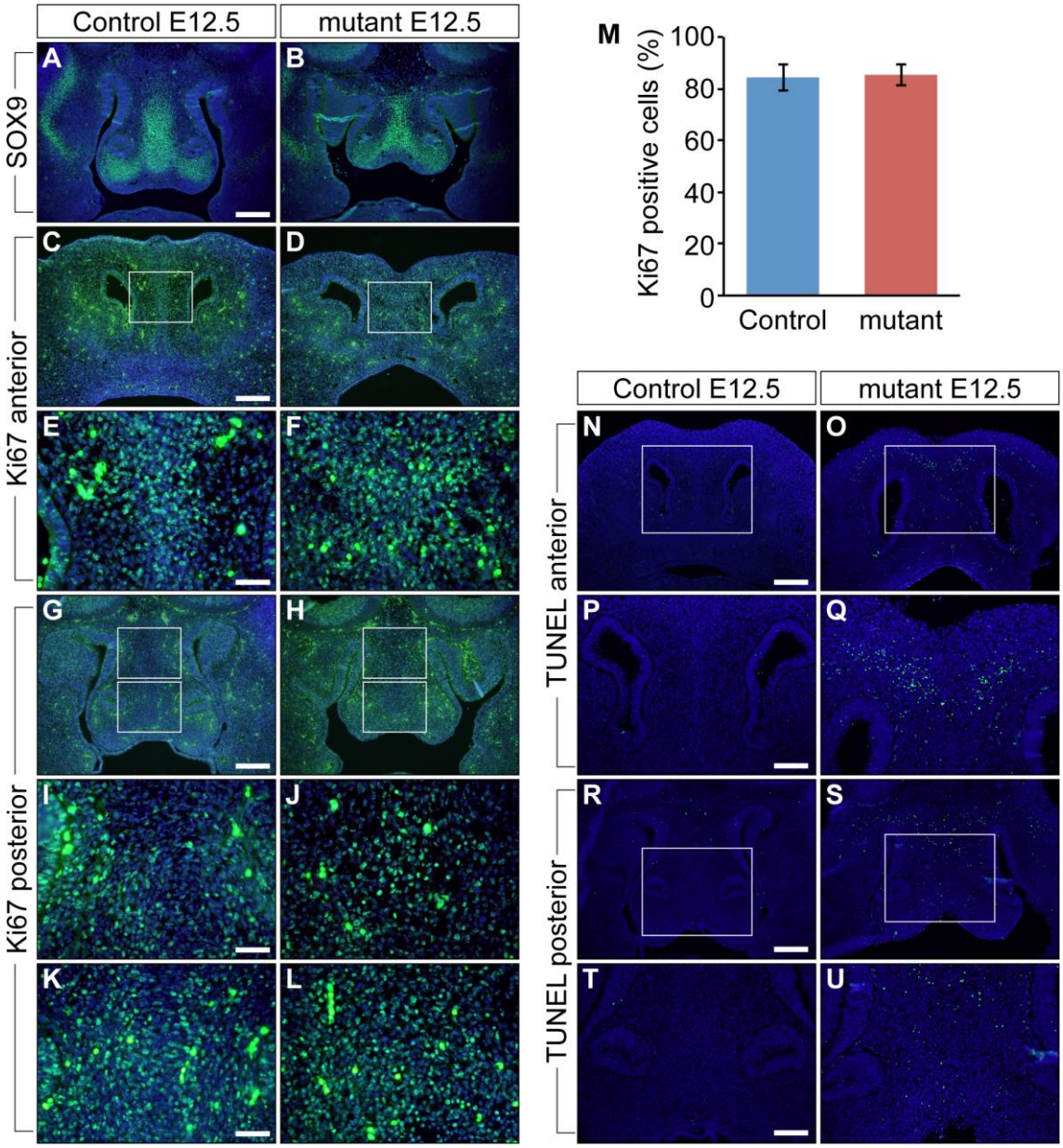

Supplementary Figure 3. SOX9 expression, cell proliferation, and apoptosis in the developing nasal cartilage at E12.5. (**A**,**B**) Immunohistochemistry was performed using SOX9 antibody (green). The level of SOX9 was unchanged between control and mutant nasal septa. Scale bar: 200 μm. (**C**-**L**) Immunohistochemistry using Ki67 antibody (green). Ki67 positive nuclei are visualized as green in the anterior (C-F) and the posterior nasal cavities (G-L) at E12.5. Boxed areas in C,D,G, and H are shown at higher magnification in E,F,I (upper box in G),K (lower box in G),J (upper box in H) and L (lower box in H) respectively. Scale bars in C,G: 200 μm. E,I,K: 50 μm. (**M**) The ratio of Ki67-positive cell number to total cell number was compared between controls

and mutants. Cell number was counted in high-magnification images (*n=5*). All data are represented as mean ± SD. (**N-U**) TUNEL assay using E12.5 control (N,P,R,T) and mutant (O,Q,S,U) frontal sections. Nuclei of apoptotic cells were shown in green. Boxed areas in N,O,R, and S are shown at high magnification in P,Q,T, and U respectively. All images are merged with DAPI staining which is shown in blue. Scale bars in N,R: 200 μm. P,T: 100 μm.

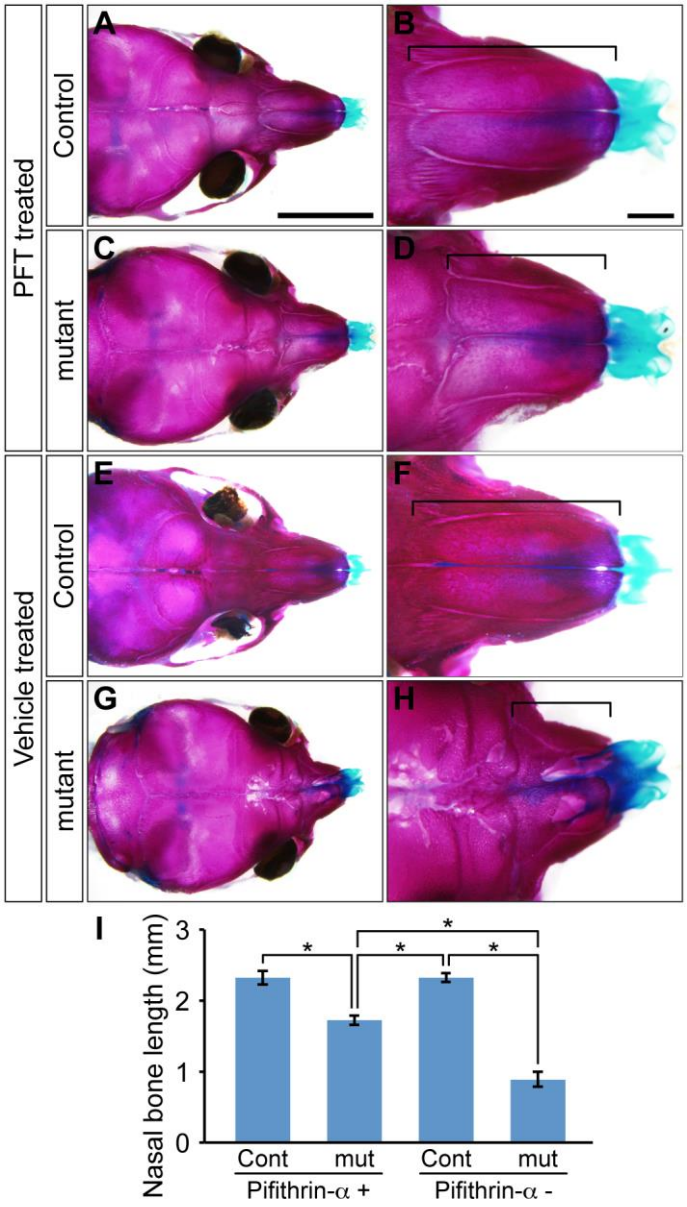

Supplementary Figure 4. Skeletal analysis of PFT and vehicle treated mutants. (**A-H**) Alcian blue and alizarin red staining was performed using PFT treated control (A,B), PFT treated mutant (C,D), vehicle treated control (E,F), and vehicle treated mutant (G,H) skulls at P10. Anteroposterior length of nasal bones was measured (B,D,E,H, brackets). Scale bars in A: 5 mm. B: 1 mm. (**I**) Comparison of nasal bone length among four groups (*n=4*). **p* < 0.001. All data are represented as mean ± SD.

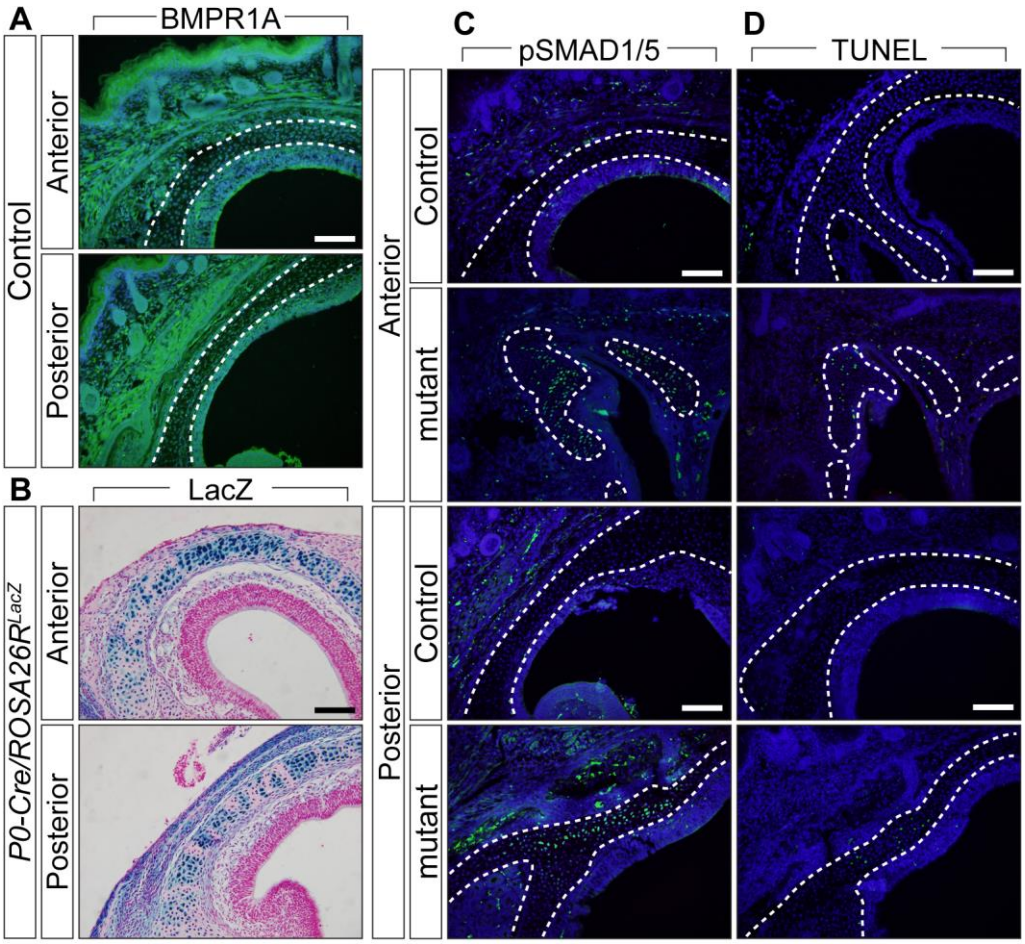

Supplementary Figure 5. Cre-induced recombination in nasal tissue correlates to levels of pSMAD1/5 and apoptosis at newborns. (**A**) Immunohistochemistry was performed using BMPR1A antibody (green). (**B**) The *P0-Cre/ROSA26R*^{LacZ} newborn mice were stained for beta-gal activity, embedded, and serially sectioned. The LacZ staining was present strongly in both the nasal cartilage and the frontal bone. (**C**) Immunohistochemistry was performed in newborn control and type 2 mutant mice using pSMAD1/5 antibody (green). (**D**) TUNEL assay using newborn control and type 2 mutant mice. Nuclei of apoptotic cells were shown in green. Blue indicates DAPI. The dashed line indicates the outline of the nasal cartilage. Scale bars in A,B,C: 100 μm.